BJPS

Brazilian Journal of Pharmaceutical Sciences

http://dx.doi.org/10.1590/s2175-97902023e21639

Article

Protective Effect of Combined Metoprolol and Atractylenolide I in Rats with Acute Myocardial Infarction via Modulation of the SIRT3 /β-CATENIN/PPAR-γ Signaling Pathway

Weijian Zhou[1§], Jing Liu[2§], Zhongli Sun[3,4], Yongpeng Dong[5], Meiming Zhu[6], Li Li[7*]

[1]Department of Cardiology, Weihai Municipal Hospital, Weihai, Shandong, China, [2]Department of Cardiology, Yantai Affiliated Hospital of Binzhou Medical University, Binzhou, Shandong, China, [3]Department of Pharmacy, Liaocheng People's Hospital, Liaocheng, Shandong, China, [4]Key Laboratory of Clinical Pharmacology, Liaocheng People's Hospital, Liaocheng, Shandong, China, [5]ECG Room, Binzhou Hospital of Traditional Chinese Medicine, Binzhou, Shandong, China, 6Weiji Town Health Center, Binzhou, Shandong, China, 7Department of Geriatrics, Zibo Central Hospital, Zibo, Shandong, China

[§]Both authors contributed equally to this work and should be considered as equal first coauthors

Herein, we examined the protective effect of metoprolol combined with atractylenolide I (Atr I) in acute myocardial infarction (AMI) by regulating the SIRT3 (silent information regulator 3)/β-catenin/peroxisome proliferator-activated receptor gamma (PPAR-γ) signaling pathway. Briefly, 50 rats were randomly divided into the sham operation, model, metoprolol, Atr I, and combination metoprolol with Atr I groups (combined treatment group). The AMI model was established by ligating the left anterior descending coronary artery. After treatment, infarct size, histopathological changes, and cell apoptosis were examined using 2,3,5-triphenyltetrazolium chloride staining, hematoxylin-eosin staining, and the TUNEL assay. The left ventricular ejection fraction (LVEF), left ventricular fraction shortening (LVFS), and left ventricular mass index (LVMI) were detected by echocardiography. Endothelin-1 (ET-1), nitric oxide (NO), tumor necrosis factor-alpha (TNF-α), and interleukin-6 (IL-6) levels were detected using enzyme-linked immunosorbent assays. Furthermore, we measured lactate dehydrogenase (LDH), creatine kinase (CK) isoenzyme (CK-MB), and CK levels. Western blotting was performed to determine the expression of SIRT3, β-catenin, and PPAR-γ. Herein, the combined treatment group exhibited increased levels of LVEF, LVFS, and NO, whereas LVMI, ET-1, TNF-α, IL-6, LDH, CK-MB, and CK levels were decreased. Importantly, the underlying mechanism may afford protection against AMI by increasing the expression levels of SIRT3, β-catenin, and PPAR-γ.

Keywords: Acute myocardial infarction. Metoprolol. Atractylenolide I. SIRT3/β-Catenin/PPAR-γ pathway.

INTRODUCTION

Acute myocardial infarction (AMI), a type of myocardial necrosis, is caused by acute and persistent ischemia and hypoxia of the coronary arteries (Chen *et al*., 2016; Sheu *et al*., 2019). Most clinical manifestations are severe, presenting as persistent retrosternal pain accompanied by elevated serum myocardial enzyme activity and potentially complicated by arrhythmia, shock, or heart failure (Posma *et al*., 2019). AMI is a widespread disease that impairs the safety of human life (Zhao *et al*., 2020). Importantly, the incidence of AMI in China has shown a notable upward trend.

***Correspondence:** L. Li. Department of Geriatrics. Zibo Central Hospital, No. 54. Gongqingtuanxi Road, Zhangdian District. Zibo, Shandong 255036, China. Phone: +86-0533-2360433. Email: lili5li@163.com. ORCID: https://orcid.org/0000-0002-5468-6875. **Authors email:** W. Zhou - email: 18663118790@163.com | J. Liu - email: 123804599@qq.com | Z. Sun - email: sunzlhktk@126.com | Y. Dong - email: 360057108@qq.com | M. Zhu - email: 1443621873@qq.com | L. Li - email: lili5li@163.com

Currently, it is estimated that approximately 2 million individuals suffer from AMI in China, with at least half a million new patients diagnosed annually (Wu *et al*., 2021). AMI is a pathophysiological process involving myocardial tissue structure, ventricular size, morphology, and functional changes (Yang *et al*., 2021). It is the main pathophysiological mechanism underlying progressive changes in cardiac function post-myocardial infarction and is mainly related to the overexpression of inflammatory cytokines, neuroendocrine regulation, and excessive activation of oxidative stress (Meng *et al*., 2021). Currently, the principal drugs employed to treat AMI include rosuvastatin, enteric-coated aspirin tablets, and dopamine (Fei *et al*., 2016; Sun *et al*., 2020; Zhou *et al*., 2021). However, these therapeutic agents are known to be associated with serious side effects, thereby reducing their clinical efficacy.

As a β_1 receptor blocker, metoprolol plays a pivotal role in preventing and treating myocardial infarction (Clemente-Moragón *et al*., 2020; Norhayati *et al*., 2020; Zaatari *et al*., 2021). Atractylenolide I (Atr I), a sesquiterpenoid, is isolated from atractylodisatractylodis (Yu *et al*., 2016; Sun *et al*., 2021). Atr I reportedly exerts potent anti-inflammatory (Ji, Chen, Zheng, 2014), antioxidant (Deng *et al*., 2021), and neuroprotective activities (More, Choi, 2017). However, the role of Atr I in myocardial infarction remains poorly explored. Moreover, there is no available evidence regarding the potential cardioprotective effect afforded by co-administering metoprolol and Atr I.

SIRT3 (silent information regulator 3) is extensively used to treat myocardial injury (Lv *et al*., 2021). SIRT3 is primarily located in mitochondria and is critical in regulating cellular energy metabolism and oxidative stress (Lee *et al*., 2021). B-catenin promotes transdifferentiation of myocardial fibroblasts and can induce myocardial damage (Piven, Winata, 2017; Li *et al*., 2020). Peroxisome proliferator-activated receptor gamma (PPAR-γ), as a member of the nuclear receptor transcription factor superfamily, is known to inhibit cardiomyocyte injury (Mohamed Kamel, 2021; Paciello *et al*., 2021). Furthermore, β-catenin can directly regulate PPAR expression in cardiomyocytes and is regulated by SIRT3 (Song *et al*., 2019).

Considering the changes observed in the SIRT3/β-catenin/PPAR-γ signaling pathway during the development of AMI, we examined the role and mechanism of metoprolol and Atr I in myocardial infarction in the present study using AMI model rats to establish an experimental basis for rational and efficient clinical drug utilization.

MATERIAL AND METHODS

Material

Metoprolol was supplied by Chongqing Tingyi Biotechnology Co. Ltd. Atr I was purchased from Shanghai Jiwei Biotechnology Co., Ltd. Endothelin-1 (ET-1), nitric oxide (NO), tumor necrosis factor-alpha (TNF-α), interleukin-6 (IL-6), lactate dehydrogenase (LDH), creatine kinase (CK) isoenzyme (CK-MB), and CK were acquired from Shanghai Xinyu Biotechnology Co. Ltd. The TUNEL staining kit was purchased from Shanghai Yaji Biotechnology Co. Ltd. All antibodies, including SIRT3, β-catenin, and PPAR-γ, were obtained from Wuhan Feien Biotechnology Co. Ltd.

Male Sprague Dawley rats (6-7 week-old, 200 ± 20 g) were supplied by the Laboratory Animal Center. The rats were reared adaptively for one week prior to experimentation, with free access to food and water during the experiment. All applicable international, national, and institutional guidelines for the care and use of animals were followed. This study was approved by the Ethics Committee of the Zibo Central Hospital.

Modeling and administration methods

The AMI model was established by ligating the left anterior descending coronary artery. Rats were intraperitoneally administered anesthesia using 3 mL/kg chloral hydrate. Disinfection was performed using iodophor. The skin of the neck was incised, and the subcutaneous tissue and muscles were separated. The fourth rib was cut, the chest was opened, the pericardium was cut, and the heart was exposed. The anterior descending coronary artery was ligated at approximately 2 mm from the lower edge of the left atrial appendage.

After 20 min, the left ventricular anterior wall was pale, and contractility was weakened. Considering the sham operation group, the thread was placed without ligation. Post-surgery, penicillin (40,000 U) was administered intramuscularly for three days to prevent wound infection.

Fifty rats were randomly separated into five groups: the sham operation group, AMI group, metoprolol group, Atr I group, and combined treatment group. Metoprolol, Atr I, and combined treatment group rats were orally administered metoprolol (8 mg/kg), Atr I (4 mg/kg), and metoprolol (8 mg/kg) + Atr I (4 mg/kg). The sham and AMI rats were administered physiological saline continuously for 28 days.

2,3,5-Triphenyltetrazolium chloride (TTC) staining determined myocardial infarct size

After euthanizing the rats, the heart was harvested quickly, and the aorta was intubated. The heart was then flushed with phosphate-buffered saline (PBS), and TTC was injected into the aorta, followed by incubation at 37°C for 30 min. The necrotic myocardium was white, and the non-necrotic myocardium was red. Prepared specimens were stored at -80°C for 10 min, sliced (1.0 mm thick), and fixed overnight with 10% formaldehyde solution. ImageJ software (National Institutes of Health, Bethesda, MD) was used to calculate the left ventricular myocardial necrosis area and total left ventricular area. Percentage of myocardial infarction area = left ventricular myocardial necrosis area/total left ventricular area × 100%.

Echocardiographic examination

After treatment, rats were anesthetized intraperitoneally with 1% pentobarbital sodium (40 mg/kg) and fixed on their backs. High-resolution ultrasound (Shanghai Yuyan Scientific Instrument Co., Ltd) was used to detect left ventricular ejection fraction (LVEF) and left ventricular fraction shortening (LVFS) to further evaluate cardiac function. Next, the right ventricular wall and atrium were excised, and the left ventricle and ventricular septum were preserved. The left ventricular mass index (LVMI) was calculated by precise weighing with a balance.

Hematoxylin and eosin (HE) staining

Following ultrasound examination, the rats were euthanized. The heart was harvested by thoracotomy. The left heart tissue was cut into 5-mm thin sections and fixed with paraformaldehyde for 10 min. Slices were decolorized with ethanol, dehydrated with xylene, and sealed with neutral glue. Histopathological changes were observed under a microscope.

TUNEL assay

After the final administration, the rats were sacrificed, and their hearts were dissected to separate the myocardial tissue at the infarct site. The left heart tissue was fixed with 4% paraformaldehyde and then embedded in paraffin. The specimens were dehydrated and embedded in 30% sucrose. After TUNEL staining, fluorescence microscopy was used to observe and obtain images.

Determination of myocardial enzyme content

After the final treatment, heart tissue was harvested and ground in PBS. The supernatant was centrifuged at 12000 rpm for 10 min and stored at -80°C. The respective kit was used to detect LDH, CK, and CK-MB levels.

Enzyme-linked immunosorbent assay (ELISA) detection

Twenty-four hours after the last administration, blood was collected from the retroorbital venous plexus of rats. After standing for 30 min, the whole blood was centrifuged at 12000 rpm for 10 min. After absorbing the supernatant, the levels of ET-1, NO, TNF-α, and IL-6 were measured using ELISA kits.

Western blot detection

Briefly, myocardial tissue was harvested from the infarct site. Non-myocardial tissues, including blood vessels and fat, were removed to isolate the left ventricle. Total protein was extracted using RIPA lysate and quantified. The total protein (50 μg) from each protein sample was used

for western blot analysis. Protein samples were added to a polyacrylamide gel for electrophoresis and film transfer. Subsequently, the nitrocellulose membrane was placed in 5% skim milk, sealed at room temperature for 2 h, and thrice washed with TBST (Tris-buffered saline, 0.1% Tween 20). SIRT3 (1:100), anti-β-catenin (1:200), and PPAR γ (1:1000) antibodies were incubated overnight at 4°C. Next, the corresponding horseradish peroxidase-labeled secondary antibody (1:1000) was diluted and incubated at room temperature for 1 h. The specimens were developed in a darkroom using ECL reagent, and the image was scanned using a Bio-Rad gel electrophoresis image analysis system. The relative intensities of protein bands were analyzed using the Quantity One software (Bio-Rad Laboratories, Hercules, CA, USA).

Statistical analysis

Data were statistically analyzed using SPSS software (version 20.0; IBM Corp., Armonk, NY, USA). Data are presented as x ± s. One-way analysis of variance (ANOVA) was used for multi-group comparisons. A p-value of <0.05 was deemed a significant difference.

RESULTS

Assessment of cardiac function

Herein, cardiac function was examined using echocardiography. The model group exhibited markedly reduced LVEF and LVFS, whereas LVMI was substantially increased, thereby indicating the occurrence of left ventricular remodeling to a certain extent after AMI (Figure 1, p <0.01). LVEF and LVFS were dramatically enhanced, and LVMI was notably reduced in the metoprolol, Atr I, and combined treatment groups (p <0.05, p <0.01). Moreover, the impact of combined treatment was superior to that of metoprolol or Atr I administration (p <0.05). The effect of combined treatment was slightly better than that of Atr I. Considering LVEF and LVFS levels, there was no significant difference between the combined treatment and Atr I groups (Figure 1A–1 B).

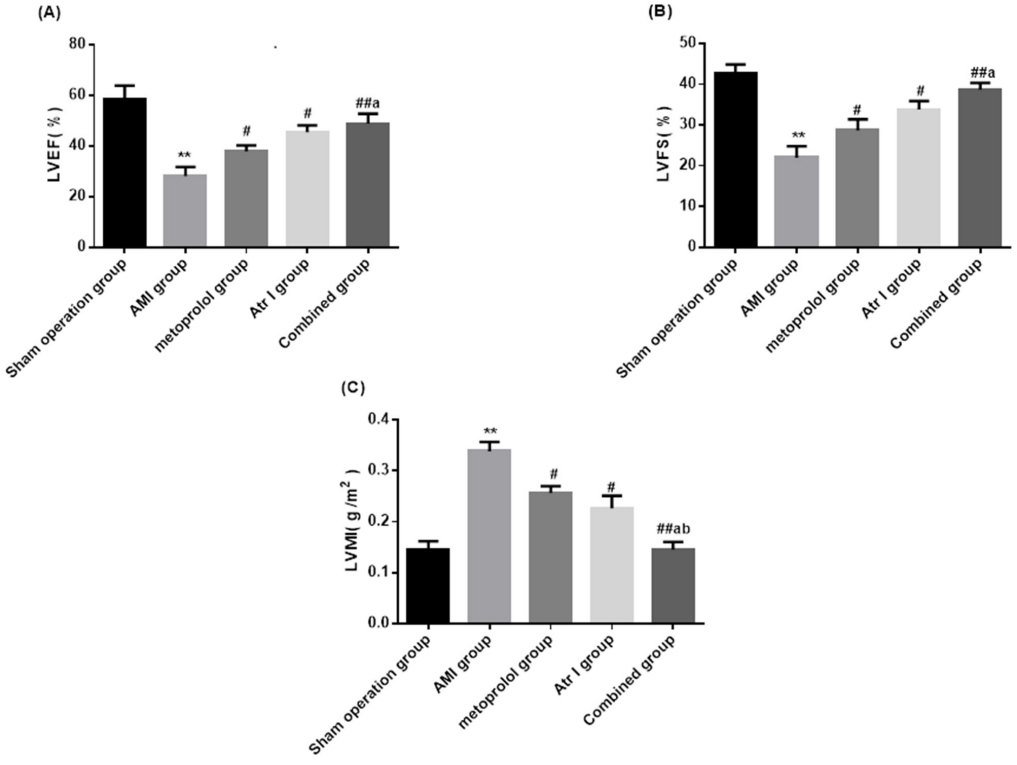

FIGURE 1 - Heart function determination. (A) LVEF, (B) LVFS, (C) LVMI. ** p 0.01 or # p <0.05, ## p <0.01 compared with the sham-operated group or AMI group, [a] p <0.05 or [b] p <0.05 compared with the metoprolol or Atr I group. AMI, acute myocardial infarction; Atr I, atractylenolide I; LVEF, left ventricular ejection fraction; LVFS, left ventricular fraction shortening; LVMI, left ventricular mass index.

Detection of areas of myocardial infarction

The sham-operated group displayed no myocardial infarction. The infarct size was substantially reduced in the Atr I and combined treatment groups (Table I, p <0.05 or p <0.01). No significant difference was observed between the metoprolol and AMI groups. The therapeutic effect of combined treatment was similar to that of Atr I. In the TTC experiment, the non-infarcted areas of the myocardium were notably brick-red, whereas infarcted areas appeared predominantly yellow-white. The combined treatment group exhibited better alleviation of myocardial infarction than the metoprolol or Atr I groups (Figure 2). The effects of Atr I were superior to those of metoprolol. Most importantly, the combined treatment group exhibited the smallest infarct area, which was restored to the level of the sham-operated group.

TABLE I - Percentage of myocardial infarction

Group	Percentage of myocardial infarction area
Sham operation group	0
AMI group	58.32 ± 2.13 **
metoprolol group	49.13 ± 2.31
Atr I group	42.87 ± 1.98 #
Combined group	37.61 ± 2.09 ##a

** $p < 0.01$ or # $p < 0.05$, ## $p < 0.01$ contrast to Sham operation group or AMI group, a $p < 0.05$ contrast to metoprolol.

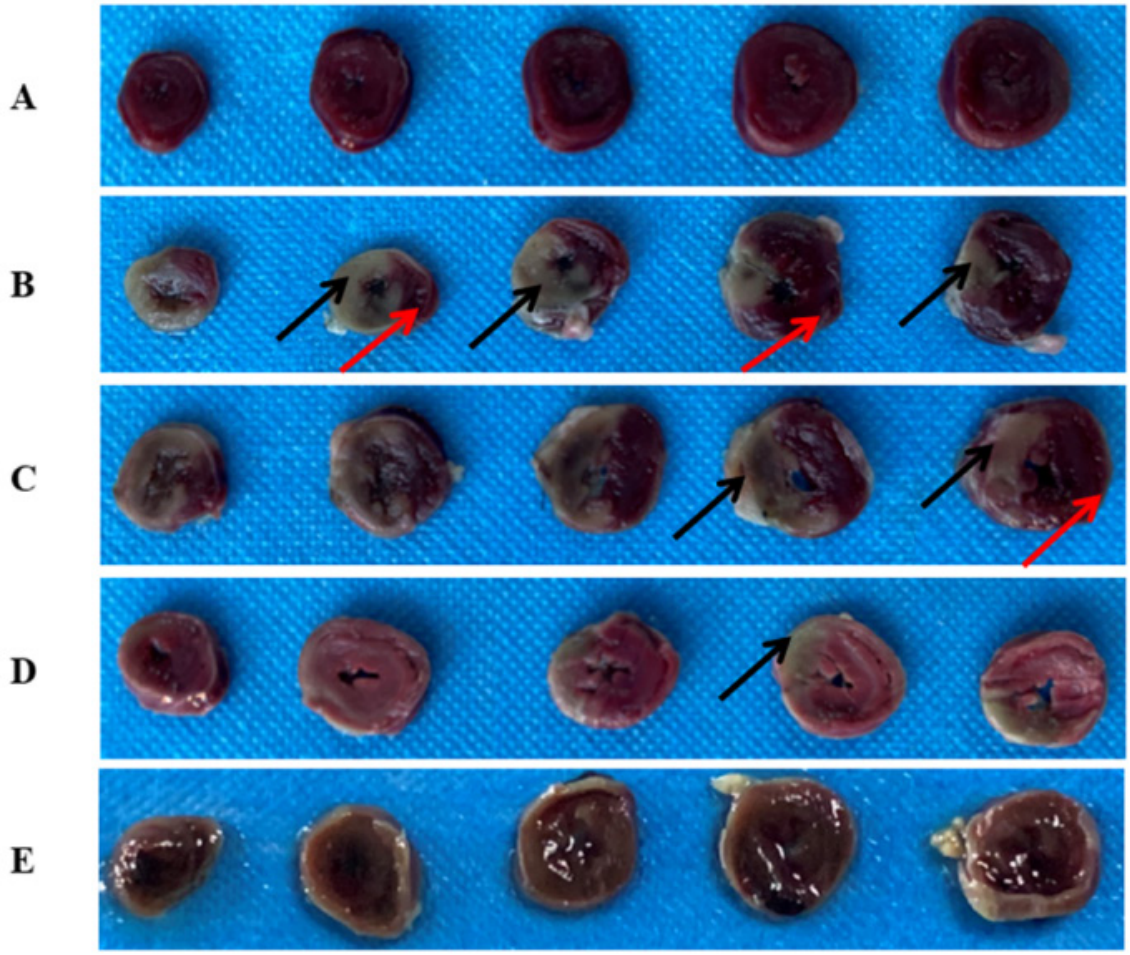

FIGURE 2 - TTC staining of myocardial tissue. (A) Sham-operated group, (B) AMI group, (C) metoprolol group, (D) Atr I group, and (E) Combined treatment group. Black arrows indicate the infarct area, and red arrows indicate the non-infarction area. AMI, acute myocardial infarction; Atr I, atractylenolide I.

Histopathological changes in myocardial tissues

In the HE staining experiment, black arrows represent cardiomyocytes, and red arrows indicate vacuoles. In the sham-operated group, myocardial cells were closely arranged without notable inflammatory cell infiltration. In the model group, the arrangement of myocardial cells was disordered, accompanied by inflammatory cell infiltration. The metoprolol, Atr I, and combined treatment could relieve the degree of myocardial necrosis (Figure 3). The combined treatment exhibited the strongest effect against cardiomyocyte injury. The effect of Atr I was slightly better than that of metoprolol. No prominent differences were detected between the metoprolol and AMI groups.

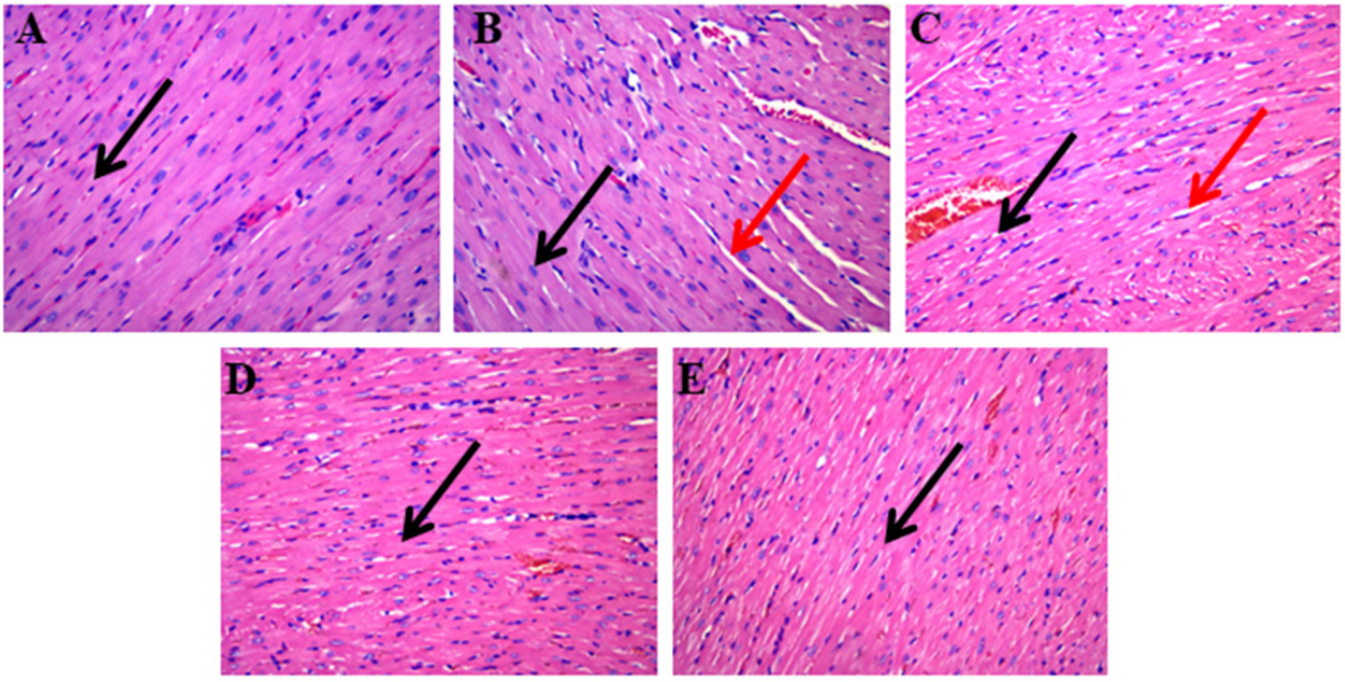

FIGURE 3 - Histopathological changes in myocardial tissue specimens (400×). (A) Sham-operated group, (B) AMI group, (C) metoprolol group, (D) Atr I group, and (E) combined treatment group. Black arrows represent cardiomyocytes, and red arrows indicate vacuoles. AMI, acute myocardial infarction; Atr I, atractylenolide I.

Detection of cell apoptosis using TUNEL

Next, we examined cardiomyocyte apoptosis using TUNEL staining. Black arrows indicate apoptotic cells, and yellow arrows indicate apoptotic cells. Based on the TUNEL analysis, the apoptosis rate of cells surrounding the myocardial infarct was elevated in the model group after AMI. Interestingly, metoprolol, Atr I, and combined treatment could reduce the apoptosis rate of cells surrounding the myocardial infarct (Figure 4). Moreover, the effect of the combined treatment was superior to that of metoprolol and Atr I alone. In addition, there were no significant differences in cardiomyocyte apoptosis between the metoprolol and AMI groups.

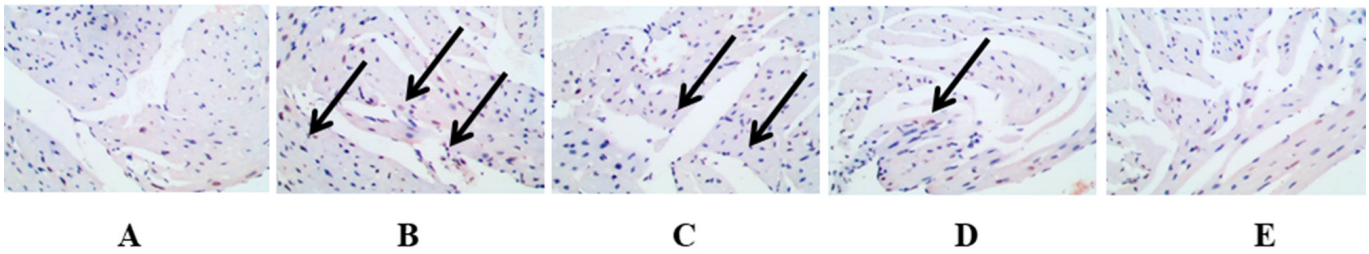

FIGURE 4 - Assessment of cardiomyocyte apoptosis using TUNEL staining (400×). (A) Sham-operated group, (B) AMI group, (C) metoprolol group, (D) Atr I group, and (E) combined treatment group. Black arrows indicate apoptotic cells, and apoptotic cells are yellow. AMI, acute myocardial infarction; Atr I, atractylenolide I.

Serum levels of inflammatory cytokines

The model group presented substantially elevated serum levels of ET-1, TNF-α, and IL-6, along with a marked reduction in NO levels (Figure 5, p <0.01). Herein, metoprolol, Atr I, and combined treatment could suppress ET-1, TNF-α and IL-6 levels and enhance NO levels (Figure 5, p <0.01). There was no significant difference between the combined treatment group and Atr I groups considering ET-1 levels (Figure 5A**)**. Notably, the combined treatment afforded the strongest effect.

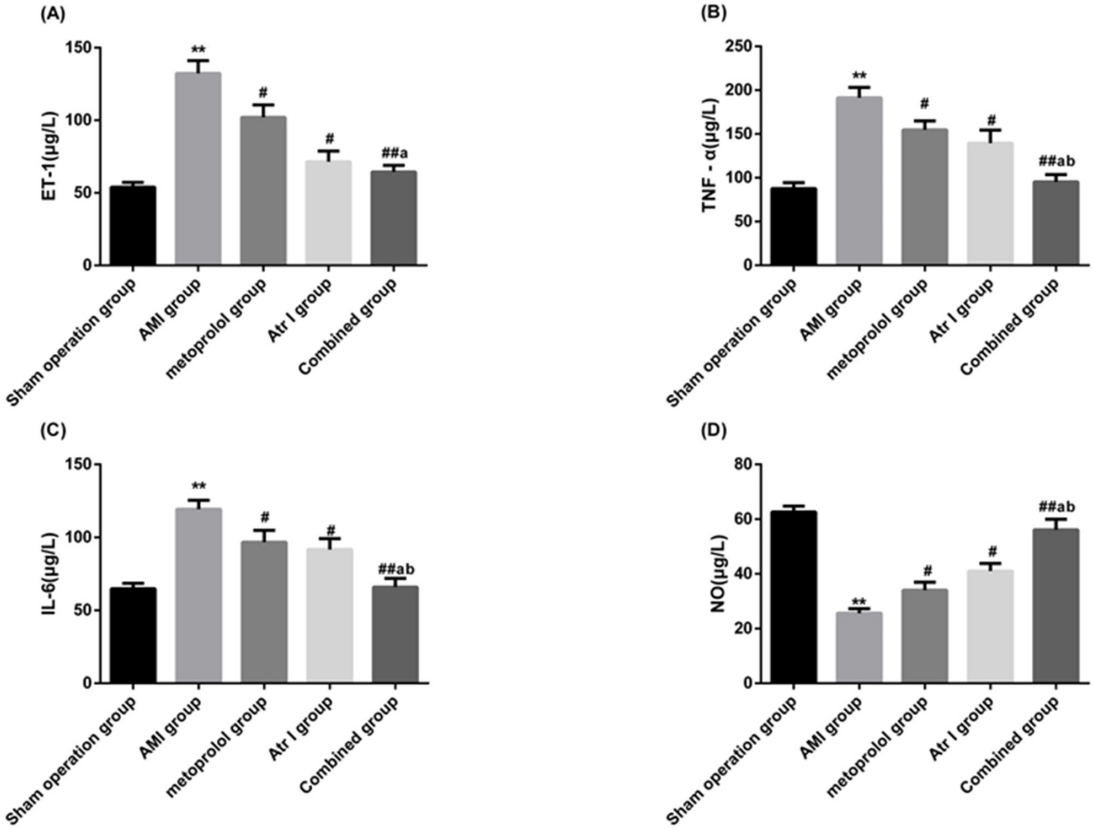

FIGURE 5 - Serum levels of inflammatory cytokines. (A) ET-1, (B) TNF-α, (C) IL-6, and (D) NO. $^{**}p$ <0.01 or $^{\#}p$ <0.05, $^{\#\#}p$ <0.01 compared with the sham-operated group or AMI group, ^{a}p <0.05 or ^{b}p <0.05 compared with the metoprolol or Atr I group. AMI, acute myocardial infarction; Atr I, atractylenolide I; ET-1, endothelin-1; IL-6, interleukin-6; NO, nitric oxide; TNF-α, tumor necrosis factor-α.

Effect of myocardial tissue on myocardial enzymes

As shown in Figure 6, levels of LDH, CK, and CK-MB were significantly elevated in the AMI group (p <0.01). Metoprolol, Atr I, and combined treatment substantially ameliorated LDH, CK, and CK-MB levels (p <0.05, p <0.01). We detected almost no difference in the CK content between the combined treatment and Atr I groups (Figure 6B). The CK-MB content exhibited an identical trend (Figure 6C). Following combined treatment, the levels of these factors were similar to those in the sham-operated group.

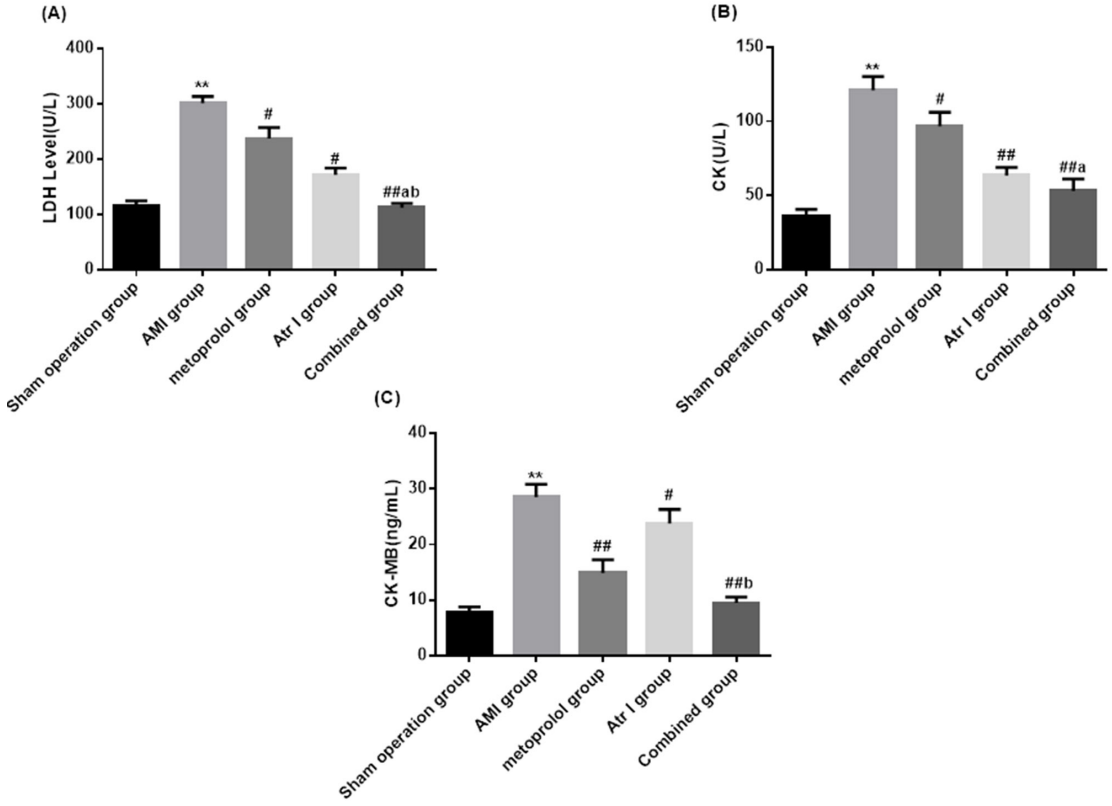

FIGURE 6 - Determination of myocardial enzymes. (A) LDH, (B) CK, and (C) CK-MB. $^{**}p$ <0.01 or $^{\#}p$ <0.05, $^{\#\#}p$ <0.01 compared with the sham-operated group or AMI group, $^{a}p < 0.05$ or $^{b}p < 0.05$ compared with the metoprolol or Atr I group. AMI, acute myocardial infarction; Atr I, atractylenolide I; CK, creatine kinase; CK-MB, creatine kinase isoenzyme LDH, lactate dehydrogenase.

Western blotting analysis

We performed western blotting to measure expression levels of SIRT3, β-catenin, and PPAR-γ in rats. As shown in Figure 7A and 7B, expression levels of SIRT3, β-catenin, and PPAR-γ were decreased in the model group ($p < 0.01$). Compared with the model group, the combined treatment group exhibited markedly increased expression levels of SIRT3, β-catenin, and PPAR γ, exceeding those of metoprolol or Atr I groups ($p < 0.01$ or $p < 0.05$). The effect of Atr I was better than that of metoprolol considering SIRT3 expression, while metoprolol afforded a better effect than Atr I considering β-catenin expression.

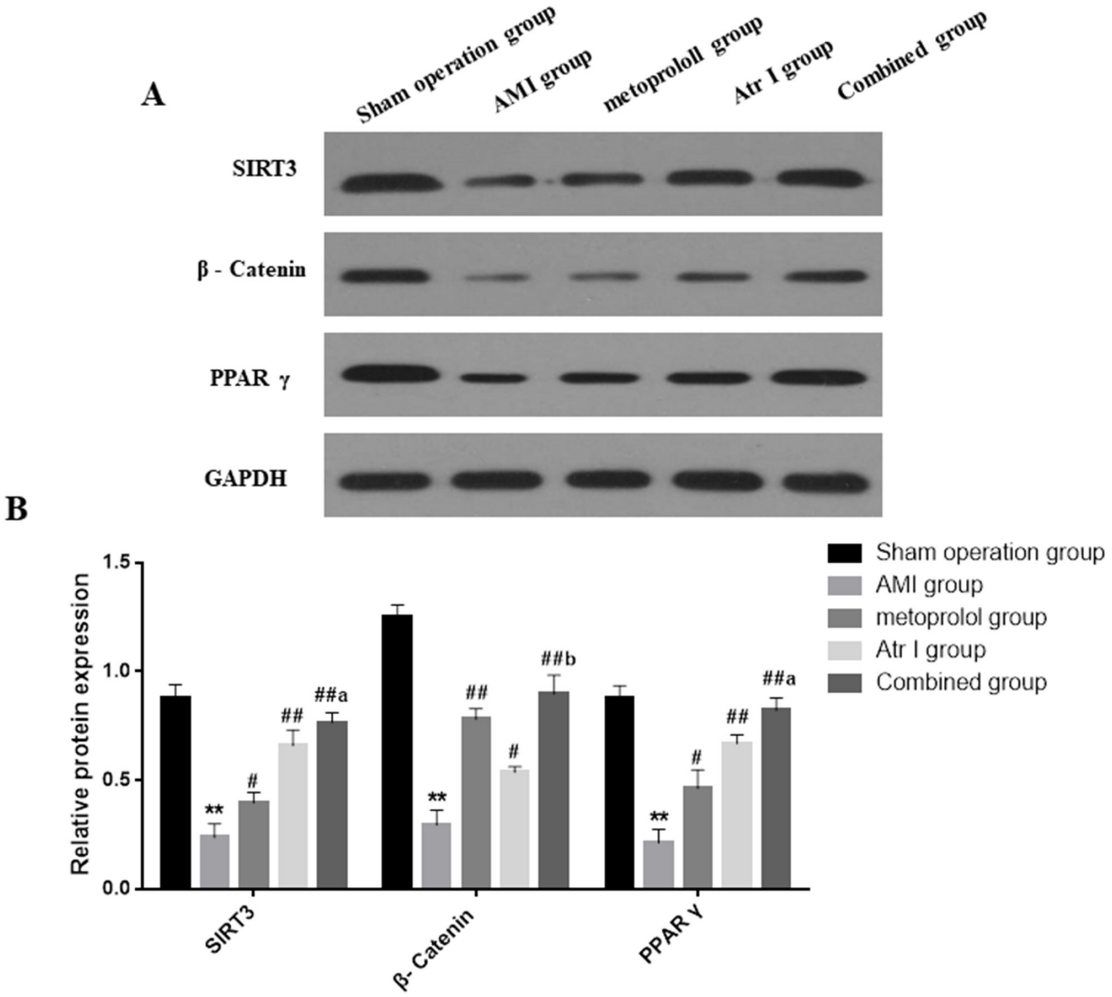

FIGURE 7 - Western blot analysis of SIRT3, β-catenin, and PPAR-γ. $^{**}p$ <0.01 or $^{\#}p$ <0.05, $^{\#\#}p$ <0.01 compared with the sham-operated group or AMI group, $^{a}p < 0.05$ or $^{b}p < 0.05$ compared with the metoprolol or Atr I group. AMI, acute myocardial infarction; Atr I, atractylenolide I; PPAR-γ, proliferator-activated receptor gamma; SIRT3, silent information regulator 3.

DISCUSSION

AMI is a common cardiovascular emergency (Sun *et al*., 2019; Sun *et al*., 2019; Zhao *et al*., 2019) characterized by myocardial necrosis, attributed to acute and continuous ischemia and hypoxia of the coronary arteries (Abel, Clark, 2021; Ishikura *et al*., 2021). Typically, this clinical syndrome occurs secondary to thrombosis due to unstable plaque rupture, erosion, and endothelial injury of the coronary artery, resulting in myocardial ischemia, injury, and necrosis (Bosco *et al*., 2021; Gao *et al*., 2021; Lin, Zheng, Jiang, 2021; Metwalli *et al*., 2021). Although AMI is most common in Western countries, its incidence in China is increasing annually (Tai *et al*., 2018; Lin, Feng, Xu, 2019). The World Health Organization predicted that AMI would be the world's largest cause of death by 2021 (Gheini, Pooria, Pourya, 2020). β-blockers are commonly used to treat AMI (Liu *et al*., 2019; Chen *et al*., 2020) and are known to antagonize the competitive binding of catecholamines and beta-adrenoceptors, thereby blocking excitatory synaptic transmission (Pesaro *et al*., 2010; DiNicolantonio *et al*., 2015). In the present study, we revealed that combined treatment with metoprolol and Atr I could afford cardioprotection in rats by activating the SIRT3/β-catenin/PPAR-γ signaling pathway, exhibiting superior effects to metoprolol and Atr I monotherapy.

Clinically, ultrasonic electrocardiography is used to examine the degree of myocardial infarction (Wang *et*

al., 2020). LVEF, LVFS, and LVMI can reflect cardiac function and adjudge abnormal changes in cardiac systolic function (Ma *et al*., 2017; Rong *et al*., 2018; Hou *et al*., 2020). Herein, we observed that combined treatment could ameliorate cardiac function by enhancing LVEF and LVFS and reducing LVMI. During myocardial infarction, coronary blood flow is disrupted, accompanied by reduced myocardial contractility (Veltman *et al*., 2021). It has been reported that myocardial contractility is closely related to the size of myocardial infarction (Zhao *et al*., 2019). In the present study, the combined treatment showed better abatement of myocardial infarction than treatment with metoprolol or Atr I alone. Importantly, the infarct area in the combined treatment group was restored to normal. Furthermore, our results revealed that the combined treatment could reduce cardiomyocyte apoptosis.

Vascular endothelial dysfunction affects fibroblast proliferation and promotes the development of myocardial infarction by secreting vasoactive substances, such as ET-1, TNF-α, IL-6, and NO (Wang *et al*., 2017; Li, Yan, 2018); these factors are deemed crucial myocardial inflammatory markers (Somasuntharam *et al*., 2016). Following myocardial infarction, these inflammatory factors indirectly reflect the inflammatory status of myocardial cells. Herein, combined treatment with metoprolol and Atr I could dramatically reduce the release of ET-1, TNF-α, and IL-6, while enhancing NO levels, thereby alleviating the AMI-induced inflammatory reaction.

Cellular active enzymes, such as LDH, CK, and CK-MB, have been employed as indicators to determine the degree of cardiomyocyte injury (Qi *et al*., 2020). An increase in these factors is known to be directly proportional to cardiomyocyte injury (Liu *et al*., 2020). Combined treatment with metoprolol and Atr I markedly reduced LDH, CK, and CK-MB levels. These results suggest that combined treatment could alleviate the degree of myocardial injury in AMI rats by suppressing the activity of myocardial enzymes.

It is well-established that myocardial tissue consists of parenchymal and stromal cells, and stromal cells are primarily cardiac fibroblasts (Zhou *et al*., 2017). SIRT3, a deacetylase, is known to regulate energy metabolism, biosynthesis, and apoptosis (Paget *et al*., 2011). In addition, SIRT3 has been closely associated with cardiovascular diseases such as myocardial hypertrophy and myocardial infarction (Wei *et al*., 2019; Maghbooli *et al*., 2020). Reportedly, PPAR-γ can ameliorate heart failure and participates in ventricular remodeling (Xu *et al*., 2017). As a key factor in the Wnt signaling pathway, β-catenin promotes the transformation of cardiac fibroblasts and leads to myocardial fibrosis (Albrecht-Schgoer *et al*., 2012). Furthermore, both β-catenin and PPAR-γ can regulate each other and can be directly related to PPAR-γ (Yin *et al*., 2011). In the present study, combined treatment with metoprolol and Atr I markedly enhanced the expression of SIRT3, and SIRT3 could activate PPAR-γ, thus protecting cardiomyocytes. This was mainly reflected in two aspects: combined treatment not only alleviated myocardial histopathological changes, but also suppressed cardiomyocyte apoptosis.

In summary, combined treatment with metoprolol and Atr I could inhibit the inflammatory response in rats with AMI and suppress cardiomyocyte apoptosis, thereby exerting a cardioprotective role in AMI. The underlying mechanism may be related to the activated SIRT3/β-catenin/PPAR-γ signaling pathway in AMI, which will afford a new research direction for preventing and treating myocardial infarction.

ACKNOWLEDGEMENTS

None.

DISCLOSURE STATEMENTS

No conflict of interest.

FUNDING

No funds, grants, or other support was received.

AUTHOR CONTRIBUTIONS

In this work, Weijian Zhou, Jing Liu and Li Li conceived the study and designed the experiments. Zhongli Sun, Yongpeng Dong and Meiming Zhu contributed to the data collection, performed the data analysis and interpreted the results. Weijian Zhou and

Jing Liu wrote the manuscript; Li Li contributed to the critical revision of article. All authors read and approved the final manuscript.

REFERENCES

Abel AAI, Clark AL. Long-term pharmacological management of reduced ejection fraction following acute myocardial infarction: Current status and future prospects. Int J Gen Med. 2021;14:7797-805.

Albrecht-Schgoer K, Schgoer W, Holfeld J, Theurl M, Wiedemann D, Steger C, et al. The angiogenic factor secretoneurin induces coronary angiogenesis in a model of myocardial infarction by stimulation of vascular endothelial growth factor signaling in endothelial cells. Circulation. 2012;126(21):2491-501.

Bosco E, Hsueh L, McConeghy KW, Gravenstein S, Saade E. Major adverse cardiovascular event definitions used in observational analysis of administrative databases: a systematic review. BMC Med Res Methodol. 2021;21(1):241.

Chen W, Spitzl A, Mathes D, Nikolaev VO, Werner F, Weirather J, et al. Endothelial actions of ANP enhance myocardial inflammatory infiltration in the early phase after acute infarction. Circ Res. 2016;119(2):237-48.

Chen Y, Tang XF, Gao RL, Yang YJ, Xu B, Yuan JQ. Association of β-Blocker therapy at discharge with clinical outcomes after acute coronary syndrome in patients without heart failure. Cardiovasc Ther. 2020;2020:4351469.

Clemente-Moragón A, Gómez M, Villena-Gutiérrez R, Lalama DV, García-Prieto J, Martínez F, et al. Metoprolol exerts a non-class effect against ischaemia-reperfusion injury by abrogating exacerbated inflammation. Eur Heart J. 2020;41(46):4425-40.

Deng M, Chen H, Long J, Song J, Xie L, Li X. Atractylenolides (I, II, and III): a review of their pharmacology and pharmacokinetics. Arch Pharm Res. 2021;44(7):633-54.

DiNicolantonio JJ, Fares H, Niazi AK, Chatterjee S, D'Ascenzo F, Cerrato E, et al. β-Blockers in hypertension, diabetes, heart failure and acute myocardial infarction: a review of the literature. Open Heart. 2015;2(1):e000230.

Fei L, Zhang J, Niu H, Yuan C, Ma X. Effects of Rosuvastatin and MiR-126 on myocardial injury induced by acute myocardial infarction in rats: Role of vascular endothelial growth factor A (VEGF-A). Med Sci Monit. 2016;22:2324-34.

Gao L, Lu D, Xia G, Zhang H. The relationship between arterial stiffness index and coronary heart disease and its severity. BMC Cardiovasc Disord. 2021;21(1):527.

Gheini A, Pooria A, Pourya A. Evaluating mortality rate and associated parameters in patients with acute coronary syndrome. Cardiovasc Hematol Disord Drug Targets. 2020;20(3):221-6.

Hou J, Chen Y, Ma D, Wang C, Jin H, An Y, et al. [Effect of chronic emotional stress induced by empty bottle stimulation on inflammatory factors in rats with acute myocardial infarction: analysis of the CXCL12/CXCR4 axis]. Nan Fang Yi Ke Da Xue Xue Bao. 2020;40(5):624-31.

Ishikura K, Nakagawa Y, Nakagawa Y, Tsuchiya A, Noda T, Takayama H, et al. The evaluation of helicopter emergency medical services with a physician for acute myocardial infarction in japan: a registry-based study of prognosis and time reduction. Air Med J. 2021;40(6):399-403.

Ji G, Chen R, Zheng J. Atractylenolide I inhibits lipopolysaccharide-induced inflammatory responses via mitogen-activated protein kinase pathways in RAW264.7 cells. Immunopharmacol Immunotoxicol. 2014;36(6):420-5.

Lee S, Jeon YM, Jo M, Kim HJ. Overexpression of SIRT3 suppresses oxidative stress-induced neurotoxicity and mitochondrial dysfunction in dopaminergic neuronal cells. Exp Neurobiol. 2021;30(5):341-55.

Li X, Yan B. Research on the effect of cytokine concentration on the immune level and survival conditions of elderly patients with sepsis. Exp Ther Med. 2018;16(2):842-6.

Li Z, Zhu S, Liu Q, Wei J, Jin Y, Wang X, et al. Polystyrene microplastics cause cardiac fibrosis by activating Wnt/β-catenin signaling pathway and promoting cardiomyocyte apoptosis in rats. Environ Pollut. 2020;265(Pt A):115025.

Lin B, Feng D, Xu J. Cardioprotective effects of microRNA-18a on acute myocardial infarction by promoting cardiomyocyte autophagy and suppressing cellular senescence via brain derived neurotrophic factor. Cell Biosci. 2019;9:38.

Lin B, Zheng W, Jiang X. Crosstalk between Circulatory Microenvironment and vascular endothelial cells in acute myocardial infarction. J Inflamm Res. 2021;14:5597-610.

Liu J, Sun G, He Y, Song F, Chen S, Guo Z, et al. Early β-blockers administration might be associated with a reduced risk of contrast-induced acute kidney injury in patients with acute myocardial infarction. J Thorac Dis. 2019;11(4):1589-96.

Liu ZF, Hu WW, Li R, Gao Y, Yan LL, Su N. Expression of lncRNA-ANRIL in patients with coronary heart disease before and after treatment and its short-term prognosis predictive value. Eur Rev Med Pharmacol Sci. 2020;24(1):376-84.

Lv D, Luo M, Cheng Z, Wang R, Yang X, Guo Y, et al. Tubeimoside i ameliorates myocardial ischemia-reperfusion

injury through sirt3-dependent regulation of oxidative stress and apoptosis. Oxid Med Cell Longev. 2021;2021:5577019.

Ma J, Li ZY, Liang XP, Guo CX, Lu PP, Ma LH. Xinfuli granule improves post-myocardial infarction ventricular remodeling and myocardial fibrosis in rats by regulating TGF-β/Smads signaling pathway. J Geriatr Cardiol. 2017;14(5):301-7.

Maghbooli Z, Emamgholipour S, Aliakbar S, Amini M, Gorgani-Firuzjaee S, Hossein-Nezhad A. Differential expressions of SIRT1, SIRT3, and SIRT4 in peripheral blood mononuclear cells from patients with type 2 diabetic retinopathy. Arch Physiol Biochem. 2020;126(4):363-8.

Meng Z, Zhao Y, Zheng X, He Y. The relationship between AKI in patients with STEMI and Short-Term mortality: A propensity score matching analysis. Angiology. 2021;72(8):733-9.

Metwalli O, Hashem E, Ajabnoor MA, Sr., Alama N, Banjar ZM. Study of some inflammatory mediators in the serum of patients with atherosclerosis and acute myocardial infarction. Cureus. 2021;13(10):e18450.

Mohamed Kamel GA. Vinpocetine attenuates fluoxetine-induced liver damage in rats; Role of Nrf2 and PPAR-γ. Hum Exp Toxicol. 2021;40(12_suppl):S509-18.

More S, Choi DK. Neuroprotective role of Atractylenolide-I in an In Vitro and In Vivo Model of Parkinson's Disease. Nutrients. 2017;9(5):451.

Norhayati MN, Shaiful Bahari I, Zaharah S, Nik Hazlina NH, Mohammad Aimanazrul Z, Irfan M. Metoprolol for prophylaxis of postoperative atrial fibrillation in cardiac surgery patients: systematic review and meta-analysis. BMJ Open. 2020;10(10):e038364.

Paciello F, Pisani A, Rolesi R, Escarrat V, Galli J, Paludetti G, et al. Noise-Induced cochlear damage involves PPAR Down-Regulation through the Interplay between oxidative stress and inflammation. Antioxidants (Basel). 2021;10(8):1188.

Paget MB, Murray HE, Bailey CJ, Flatt PR, Downing R. Rotational co-culture of clonal β-cells with endothelial cells: effect of PPAR-γ agonism in vitro on insulin and VEGF secretion. Diabetes Obes Metab. 2011;13(7):662-8.

Pesaro AE, de Matos Soeiro A, Serrano CV, Giraldez RR, Ladeira RT, Nicolau JC. Effect of beta-blockers on the risk of atrial fibrillation in patients with acute myocardial infarction. Clinics (Sao Paulo). 2010;65(3):265-70.

Piven OO, Winata CL. The canonical way to make a heart: β-catenin and plakoglobin in heart development and remodeling. Exp Biol Med (Maywood). 2017;242(18):1735-45.

Posma JJ, Grover SP, Hisada Y, Owens AP, 3rd, Antoniak S, Spronk HM, et al. Roles of coagulation proteases and PARs (Protease-Activated Receptors) in mouse models of inflammatory diseases. Arterioscler Thromb Vasc Biol. 2019;39(1):13-24.

Qi X, Sun X, Li X, Kong D, Zhao L. Significance changes in the levels of myocardial enzyme in the child patients with Mycoplasma Pneumoniae Pneumonia. Cell Mol Biol (Noisy-le-grand). 2020;66(6):41-5.

Rong SL, Wang XL, Wang YC, Wu H, Zhou XD, Wang ZK, et al. Anti-inflammatory activities of hepatocyte growth factor in post-ischemic heart failure. Acta Pharmacol Sin. 2018;39(10):1613-21.

Sheu JJ, Hsiao HY, Chung SY, Chua S, Chen KH, Sung PH, et al. Endothelial progenitor cells, rosuvastatin and valsartan have a comparable effect on repair of balloon-denudated carotid artery injury. Am J Transl Res. 2019;11(3):1282-98.

Somasuntharam I, Yehl K, Carroll SL, Maxwell JT, Martinez MD, Che PL, et al. Knockdown of TNF-α by DNAzyme gold nanoparticles as an anti-inflammatory therapy for myocardial infarction. Biomaterials. 2016;83:12-22.

Song LL, Zhang Y, Zhang XR, Song YN, Dai HZ. Theacrine attenuates myocardial fibrosis after myocardial infarction via the SIRT3/β-catenin/PPARγ pathway in estrogen-deficient mice. Eur Rev Med Pharmacol Sci. 2019;23(12):5477-86.

Sun C, Li X, Wang D, Wang L. Therapeutic and diagnostic value of Caspase-12 and study of growth differentiation factor-15 in patients with acute myocar-dial infarction. Iran J Public Health. 2020;49(12):2339-47.

Sun C, Zhang X, Yu F, Liu C, Hu F, Liu L, et al. Atractylenolide I alleviates ischemia/reperfusion injury by preserving mitochondrial function and inhibiting caspase-3 activity. J Int Med Res. 2021;49(2):300060521993315.

Sun L, Jia H, Li J, Yu M, Yang Y, Tian D, et al. Cecal Gut Microbiota and Metabolites Might Contribute to the Severity of Acute Myocardial Ischemia by Impacting the Intestinal Permeability, Oxidative Stress, and Energy Metabolism. Front Microbiol. 2019;10:1745.

Sun Z, Pang S, Cui Y, Yan B. Genetic and Functional Variants Analysis of the GATA6 Gene Promoter in Acute Myocardial Infarction. Front Genet. 2019;10:1100.

Tai S, Tang JJ, Tang L, Ni YQ, Guo Y, Hu XQ, et al. Management and Outcome of Ventricular Septal Rupture Complicating Acute Myocardial Infarction: What Is New in the Era of Percutaneous Intervention? Cardiology. 2018;141(4):226-32.

Veltman D, Wu M, Pokreisz P, Claus P, Gillijns H, Caluwé E, et al. Clec4e-Receptor Signaling in Myocardial Repair After Ischemia-Reperfusion Injury. JACC Basic Transl Sci. 2021;6(8):631-46.

Wang DM, Jin JJ, Tian LM, Zhang Z. MiR-195 promotes myocardial fibrosis in MI rats via targeting TGF-β1/Smad. J Biol Regul Homeost Agents. 2020;34(4):1325-32.

Wang Y, Qi X, Wang C, Zhao D, Wang H, Zhang J. Effects of propofol on myocardial ischemia-reperfusion injury in rats with type-2 diabetes mellitus. Biomed Rep. 2017;6(1):69-74.

Wei L, Sun X, Qi X, Zhang Y, Li Y, Xu Y. Dihydromyricetin ameliorates cardiac ischemia/reperfusion injury through sirt3 activation. Biomed Res Int. 2019;2019:6803943.

Wu R, Gao W, Dong Z, Su Y, Ji Y, Liao J, et al. Plasma heat shock protein 70 is associated with the onset of acute myocardial infarction and total occlusion in target vessels. Front Cardiovasc Med. 2021;8:688702.

Xu Y, Gu Q, Liu N, Yan Y, Yang X, Hao Y, et al. PPARγ alleviates right ventricular failure secondary to pulmonary arterial hypertension in rats. Int Heart J. 2017;58(6):948-56.

Yang H, Liu S, Du H, Hong Z, Lv Y, Nie C, et al. Hydrogen attenuates myocardial injury in rats by regulating oxidative stress and NLRP3 inflammasome mediated pyroptosis. Int J Med Sci. 2021;18(14):3318-25.

Yin H, Liu Z, Li F, Ni M, Wang B, Qiao Y, et al. Ginsenoside-Rg1 enhances angiogenesis and ameliorates ventricular remodeling in a rat model of myocardial infarction. J Mol Med (Berl). 2011;89(4):363-75.

Yu R, Yu BX, Chen JF, Lv XY, Yan ZJ, Cheng Y, et al. Anti-tumor effects of Atractylenolide I on bladder cancer cells. J Exp Clin Cancer Res. 2016;35:40.

Zaatari G, Fintel DJ, Subacius H, Germano JJ, Shani J, Goldberger JJ. Comparison of metoprolol versus carvedilol after acute myocardial infarction. Am J Cardiol. 2021;147:1-7.

Zhao J, Yu H, Yan P, Zhou X, Wang Y, Yao Y. Circulating MicroRNA-499 as a diagnostic biomarker for acute myocardial infarction: A Meta-analysis. Dis Markers. 2019;2019:6121696.

Zhao M, Fan C, Ernst PJ, Tang Y, Zhu H, Mattapally S, et al. Y-27632 preconditioning enhances transplantation of human-induced pluripotent stem cell-derived cardiomyocytes in myocardial infarction mice. Cardiovasc Res. 2019;115(2):343-56.

Zhao X, Gao S, Kajigaya S, Liu Q, Wu Z, Feng X, et al. Comprehensive analysis of single-cell RNA sequencing data from healthy human marrow hematopoietic cells. BMC Res Notes. 2020;13(1):514.

Zhou Y, Wang X, Lan S, Zhang L, Niu G, Zhang G. Application of evidence-based nursing in patients with acute myocardial infarction complicated with heart failure. Am J Transl Res. 2021;13(5):5641-6.

Zhou Y, Chen P, Liu Q, Wang Y, Zhang L, Wu R, et al. Hepatoma-derived growth factor secreted from mesenchymal stem cells reduces myocardial Ischemia-reperfusion injury. Stem Cells Int. 2017;2017:1096980.

Received for publication on 04th August 2021
Accepted for publication on 22nd March 2022